MOL PHARM

MOLECULAR PHARMACOLOGY

New Insights into the Function of M4 Muscarinic Acetylcholine Receptors Gained Using a Novel Allosteric Modulator and a DREADD (Designer Receptor Exclusively Activated by a Designer Drug)[S]

Vindhya Nawaratne, Katie Leach, Nur Suratman, Richard E. Loiacono, Christian C. Felder, Blaine N. Armbruster, Bryan L. Roth, Patrick M. Sexton, and Arthur Christopoulos

Drug Discovery Biology Laboratory, Monash Institute of Pharmaceutical Sciences and Department of Pharmacology, Monash University, Melbourne, Australia (V.N., K.L., N.S., R.E.L., P.M.S., A.C.), Neuroscience, Lilly Corporate Center, Indianapolis, Indiana (C.C.F.); Millipore Inc., St. Louis, Missouri (B.N.A.); and Departments of Pharmacology and Medicinal Chemistry, University of North Carolina Chapel Hill Medical School, North Carolina (B.L.R.)

ABSTRACT

The M4 muscarinic acetylcholine (ACh) receptor (mAChR) is a potential therapeutic target but characterized by a lack of subtype-selective ligands. We recently generated "designer receptors exclusively activated by a designer drug" (DREADDs), which contained mutations of two conserved orthosteric-site residues ($Y^{113}C/A^{203}G$ in the M4 mAChR) that caused a loss of ACh activity but a gain in responsiveness to clozapine-N-oxide (CNO). The current study characterized the interactions of the wild type and the M4 DREADD with a range of agonists, antagonists, and the recently discovered M4 mAChR allosteric potentiator, 3-amino-5-chloro-6-methoxy-4-methyl-thieno[2,3-b]pyridine-2-carboxylic acid cyclopropylamide (LY2033298). LY2033298 displayed positive binding cooperativity with ACh, neutral cooperativity with the antagonist, [3H]quinuclidinyl benzilate, and agonism for activation of phosphorylated extracellular signal-regulated kinase (ERK) 1/2 at the wild-type M4 mAChR. LY2033298's cooperativity with clozapine or CNO was weakly positive with respect to binding but profoundly negative with respect to LY2033298 signaling. Although the DREADD mutations increased the binding and function of clozapine-like compounds, all other agonists lost the ability to activate the mutant; for the orthosteric agonists ACh and pilocarpine, this was due partly to a reduced affinity, whereas the affinity of LY2033298 or the atypical agonist 4-I-[3-chlorophenyl]carbamoyloxy)-2-butynyltrimethylammnonium chloride was unaltered. The interaction between LY2033298 and clozapine-like compounds reverted to neutral cooperativity on the DREADD, whereas LY2033298 caused a striking functional rescue of ACh potency and efficacy at the DREADD. These results provide conclusive evidence for the retention of a functional allosteric site on the M4 DREADD and highlight a role for residues Tyr[113] and Ala[203] in the transmission of cooperativity.

The muscarinic acetylcholine receptors (mAChRs) are members of the G protein-coupled receptor (GPCR) superfamily and mediate the majority of the actions of acetylcholine (ACh), in both the central nervous system (CNS) and the periphery (Wess et al., 2003). Within the CNS, the M1 and M4 mAChRs show a higher level of expression than the M2, M3, and M5 subtypes and have been implicated in the regulation of cognition, sensory processing, motor coordination, and attention (Wess et al., 2007). However, these mAChRs are also characterized by a very high degree of sequence conservation

ABBREVIATIONS: mAChR, muscarinic acetylcholine receptor; GPCR, G protein-coupled receptor; ACh, acetylcholine; CNS, central nervous system; ERK, extracellular signal-regulated kinase; LY2033298, 3-amino-5-chloro-6-methoxy-4-methyl-thieno[2,3-b]pyridine-2-carboxylic acid cyclopropylamide; DREADD, designer receptor exclusively activated by a designer drug; CNO, clozapine-N-oxide; WT, wild type; McN-A-343, 4-I-[3-chlorophenyl]carbamoyloxy)-2-butynyltrimethylammnonium chloride; NDMC, N-desmethyl clozapine; CHO, Chinese hamster ovary; DMEM, Dulbecco's modified Eagle medium; FBS, fetal bovine serum; pERK, phosphorylated ERK; QNB, quinuclidinyl benzilate; NMS, N-methylscopolamine; GppNHp, guanosine 5'-[β,γ-imido]triphosphate.

within the orthosteric binding site (i.e., the site on the receptor that binds its endogenous agonist) (Wess et al., 2003; Gregory et al., 2007). As a consequence, it has traditionally been very difficult to discover orthosteric agonists or antagonists, either as therapeutic agents or pharmacological tools, that selectively target M_1 or M_4 receptors in the CNS without also interacting with other receptor subtypes, especially M_2 and M_3 receptors that mediate many peripheral cholinergic side-effects (Wess et al., 2007).

One promising approach to overcome some of the difficulties associated with mAChR drug targeting is to focus on allosteric binding sites, which are topographically distinct from the orthosteric site and thus less conserved between subtypes (Christopoulos, 2002). Allosteric modulators are ligands that bind to these sites and regulate either the affinity and/or efficacy of a classic ligand interacting with the orthosteric site (Christopoulos and Kenakin, 2002; May et al., 2007a). There are now numerous examples of GPCR allosteric modulators with greater selectivity for their targets than orthosteric agonists or antagonists (May et al., 2007b). With respect to the mAChRs, we and others (Felder et al., 2004; Chan et al., 2008; Shirey et al., 2008) have recently disclosed a new class of allosteric potentiator, exemplified by LY2033298 (Fig. 1) and related compounds, which selectively enhance the actions of ACh at the M_4 mAChR to the relative exclusion of other mAChR subtypes. Moreover, LY2033298 displays in vivo efficacy in preclinical rodent models predictive of antipsychotic drug effects, suggesting that selective activation or potentiation of M_4 mAChRs may represent a novel approach to treating schizophrenia (Chan et al., 2008).

An alternative approach to selectively targeting a given GPCR to the exclusion of others is to generate a mutant receptor that does not respond to its endogenous ligand but gains responsiveness to otherwise inert biological compounds (Bishop et al., 2000; Scearce-Levie et al., 2001). If the resulting mutant GPCR retains the fidelity of the native receptor with respect to its signaling properties while being tailored to respond only to an exogenous ligand (or ligands) specific for the mutant, then one gains a powerful tool. In particular, the mutant GPCR can be introduced into a chosen cellular environment, and the resulting biological effects observed in the presence of the exogenous ligand must reflect solely the activation of the chosen receptor and no other. Moreover, this can be performed in native tissues without the possibility of unwanted activation of the mutant GPCR by the endogenous agonist. Using random mutagenesis coupled with directed molecular evolution in yeast, we recently generated such a mutant GPCR, termed a "designer receptor exclusively activated by a designer drug" (DREADD), for each of the mAChR subtypes (Armbruster et al., 2007). We identified a novel mutation of two conserved orthosteric-site residues ($Y^{113}C$ and $A^{203}G$ in the M_4 mAChR) that yielded a profound loss in potency and efficacy of ACh for activating classic second messenger pathways, but a robust gain in responsiveness to clozapine-N-oxide (CNO), a metabolite of the atypical antipsychotic agent clozapine that is otherwise biologically inert
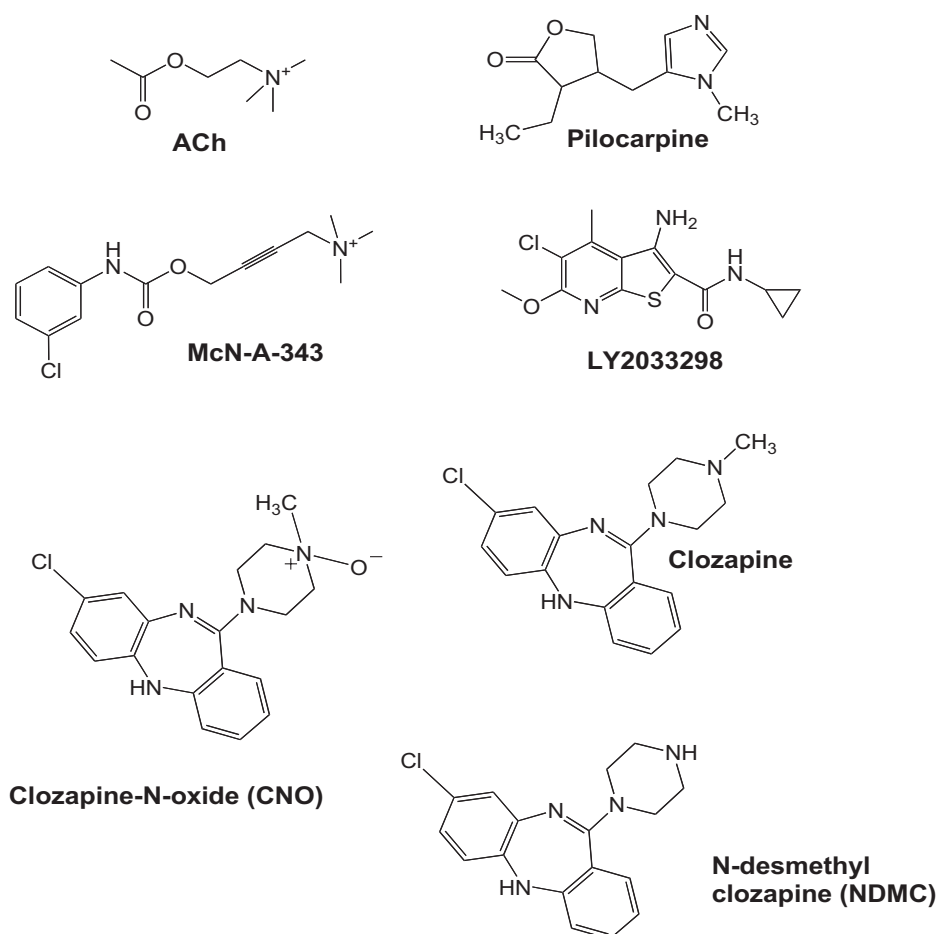

Fig. 1. Structures of compounds used in this study.

at the wild-type (WT) mAChRs. Subsequent expression of an M$_4$ DREADD into primary hippocampal neurons, followed by exposure to CNO, demonstrated its ability to induce neuronal silencing in a native environment, a property associated with ACh actions at the WT M$_4$ mAChR (Armbruster et al., 2007). This finding, supported by additional experiments examining different signaling pathways of other mAChR DREADDs (Armbruster et al., 2007), suggests that the DREADDs retain the signaling properties of native mAChRs despite losing the ability to recognize ACh, an important requirement if DREADD-based data are to be used to provide valid physiological insights.

Given that DREADDs represent a new type of reverse-engineered GPCR with significant potential as biological tools, we sought to perform a detailed characterization of the molecular pharmacology of a diverse range of orthosteric and allosteric ligands at the M$_4$ DREADD to gain further insight into the modes of activation and ligand interactions at this receptor. In addition to the classic orthosteric agonists ACh and pilocarpine, we used 4-I-[3-chlorophenyl]carbamoyloxy)-2-butynyltrimethylammnonium chloride (McN-A-343), a partial agonist that has been suggested to recognize both an allosteric and the orthosteric site on the M$_2$ mAChR (Birdsall et al., 1983; Waelbroeck, 1994; May et al., 2007a); clozapine, CNO, and N-desmethylclozapine (NDMC), a biologically active metabolite of clozapine and a functionally selective mAChR agonist (Sur et al., 2003; Davies et al., 2005); and our novel M$_4$-selective allosteric potentiator, LY2033298 (Fig. 1). We present evidence for the existence of a topographically distinct allosteric site on the M$_4$ DREADD that retains its ability to interact with orthosteric ligands but displays markedly different types of cooperative effects depending on the nature of the ligand and the receptor.

Materials and Methods

Materials. Chinese hamster ovary (CHO) Flp-In cells and Hygromycin B were purchased from Invitrogen (Carlsbad, CA). Dulbecco's modified Eagle medium (DMEM) and fetal bovine serum (FBS) were from Gibco (Gaithersburg, MD) and JRH Biosciences (Lenexa, KS), respectively. The AlphaScreen SureFire phospho-ERK1/2 reagents were kindly donated by Dr. Michael Crouch (TGR Biosciences, South Australia, Australia), whereas the AlphaScreen streptavidin donor beads and anti-IgG (protein A) acceptor beads used for phosphorylated ERK1/2 (pERK1/2) detection, [^{3}H]quinuclidinyl benzilate ([^{3}H]QNB; specific activity, 52 Ci/mmol) and [^{3}H]N-methylscopolamine ([^{3}H]NMS; specific activity, 72 Ci/mmol) were purchased from PerkinElmer Life and Analytical Sciences (Waltham, MA). NDMC and CNO were purchased from Tocris Bioscience (Bristol, UK) and BIOMOL Research Laboratories (Plymouth Meeting, PA), respectively. LY2033298 was synthesized in-house at Eli Lilly (Indianapolis, IN). All other chemicals were from Sigma Chemical Co. (St. Louis, MO).

cDNA Constructs and Generation of Stable Cell Lines. cDNA encoding the M$_4$ DREADD was generated in pcDNA3.1+ as described previously (Armbruster et al., 2007). cDNA encoding the WT M$_4$ mAChR was obtained from Missouri University of Science and Technology (http://www.cdna.org) and was provided in pcDNA3.1+. Sequences encoding the M$_4$ DREADD and WT M$_4$ mAChR were amplified by PCR and cloned into the Gateway entry vectors pDONR201 and pENTR/D-TOPO, respectively, using the BP Clonase enzyme mix and pENTR directional TOPO cloning kit, respectively, according to the manufacturer's instructions (Invitrogen). Both constructs were subsequently transferred into the Gateway destination vector pEF5/frt/v5/

dest using the LR Clonase enzyme mix (Invitrogen), and the constructs were used to transfect Flp-In CHO cells (Invitrogen) as described previously (May et al., 2007a). Cells were selected using 400 μg/ml hygromycin B to generate cell lines stably expressing each receptor construct and, after selection, were maintained in high glucose DMEM containing 10% FBS, 16 mM HEPES, and 200 μg/ml hygromycin B.

Membrane Preparations. Cells were grown until approximately 90% confluence and harvested using 2 mM EDTA in phosphate-buffered saline (137 mM NaCl, 2.7 mM KCl, 4.3 mM Na$_2$HPO$_4$, and 1.5 mM KH$_2$PO$_4$). Cells were pelleted by centrifugation for 10 min at 1200g, and the pellets were resuspended in 30 ml of buffer containing 20 mM HEPES and 10 mM EDTA at pH 7.4. All subsequent steps were performed at 4°C. The cell suspension was homogenized using a Polytron homogenizer (PT 1200 CL; Kinematica, Basel, Switzerland), with two 10-s bursts separated by cooling on ice. The cell homogenate was centrifuged for 5 min at 1700g, and the supernatant was transferred to new tubes and further centrifuged (90 min, 38,000g) in a Sorval centrifuge. The pellet was resuspended in 10 ml of buffer (20 mM HEPES and 0.1 mM EDTA, pH 7.4) and briefly homogenized to ensure uniform consistency. Membranes were aliquoted and stored at −80°C. The protein concentration was determined by the method of Bradford using bovine serum albumin as a standard (Bradford, 1976).

Radioligand Binding Assays. Saturation and competition binding assays were performed using 15 and 75 μg of membrane expressing the M$_4$ WT and DREADD receptors, respectively. For saturation binding assays, membranes were incubated with the orthosteric antagonists [^{3}H]QNB or [^{3}H]NMS in HEPES buffer (20 mM HEPES, 100 mM NaCl, and 10 mM MgCl, pH 7.4) at 37°C for 1 h before termination of the assay by rapid filtration onto GF/B grade filter paper (Whatman, Maidstone, UK) using a Brandel harvester, followed by three 2-ml washes with ice-cold NaCl (0.9%). Nonspecific binding was defined in the presence of 100 μM atropine and radioactivity was determined by liquid scintillation counting. For inhibition binding assays, membranes were incubated in HEPES buffer containing 100 μM GppNHp and increasing concentrations of the cold ligand for 3 h at 37°C in the presence of a [^{3}H]QNB concentration equal to its equilibrium dissociation constant at each receptor (0.09 and 6 nM for the WT M$_4$ mAChR and M$_4$ DREADD, respectively) as determined from saturation binding experiments. For interaction studies, competition of [^{3}H]QNB binding by ACh, clozapine, or CNO was performed in the presence of 1 and 10 μM LY2033298, the allosteric modulator. For all experiments, nonspecific binding was defined by 100 μM atropine, and the effects of vehicle were determined. The reaction was terminated and radioactivity counted as described previously.

Extracellular Signal Regulated Kinase 1/2 Phosphorylation Assays. Initial ERK1/2 phosphorylation time course experiments were performed to determine the time at which ERK1/2 phosphorylation was maximal after stimulation by each agonist. Cells were seeded into transparent 96-well plates at 4×10^4 cells per well and grown overnight or until confluent. Cells were then washed twice with phosphate-buffered saline and incubated in serum-free DMEM at 37°C for at least 4 h to allow FBS-stimulated pERK1/2 levels to subside. Cells were stimulated with agonist using a staggered addition approach. For subsequent agonist-stimulated concentration-response experiments, cells were incubated at 37°C with each agonist for the time required to generate a maximal pERK1/2 response (5 min for ACh, LY2033298, clozapine, and CNO and 8 min for pilocarpine, McN-A-343, and NDMC). For functional interaction studies, cells were incubated at 37°C with varying concentrations of agonist in the absence and presence of different concentrations of a second compound, which was added simultaneously with the agonist. For all experiments, 10% FBS was used as a positive control, and vehicle controls were also performed. The reaction was terminated by removal of drugs and lysis of cells with 100 μl of SureFire lysis buffer (as provided by the manufacturer). The lysates were agitated for 1 to 2 min and were diluted at a ratio of 4:1 (v/v) lysate/Surefire activation buffer in a total volume of 50 μl. Under low light conditions

a 1:240 (v/v) dilution of AlphaScreen beads: Surefire reaction buffer was prepared and this was mixed with the activated lysate mixture in a ratio of 6:5 (v/v), respectively, in a 384-well opaque Optiplate. Plates were incubated in the dark at 37°C for 1.5 h before the fluorescence signal was measured using a Fusion-α plate reader (PerkinElmer Life and Analytical Sciences) using standard AlphaScreen settings.

Data analysis. All data were analyzed using Prism 5.01 (GraphPad Software, San Diego, CA). For radioligand saturation binding data, nonspecific and total binding data were fitted to the following equation.

$$Y = \frac{B_{\max} \times [A]}{[A] + K_A} + NS \times [A] \tag{1}$$

where Y is radioligand binding, $B_{\max}$ is the total receptor density, $[A]$ is the radioligand concentration, K_A is the equilibrium dissociation constant of the radioligand, and NS is the fraction of nonspecific radioligand binding.

For radioligand inhibition binding experiments, specific binding of each orthosteric ligand was fitted to both a one-site (eq. 2) and a two-site (eq. 3) binding equation, and an F test was used to determine which equation better fitted the data:

$$Y = \frac{(\text{Top} - \text{Bottom})}{1 + 10^{(\log[B] - \log IC_{50})}} + \text{Bottom} \tag{2}$$

$$Y = (\text{Top} - \text{Bottom})$$
$$\times \left(\frac{\text{fraction\_1}}{1 + 10^{(\log[B] - \log IC_{50\_1})}} + \frac{1 - \text{fraction\_1}}{1 + 10^{(\log[B] - \log IC_{50\_2})}} \right) + \text{Bottom} \tag{3}$$

where Top and Bottom are the maximal and minimal asymptotes of the curve, respectively, log[B] is the concentration of inhibitor, $\log IC_{50}$ is the logarithm of the concentration of inhibitor that reduces half the maximal radioligand binding for each binding site, and fraction_1 is the proportion of high-affinity binding sites. IC_{50} values were converted to K_B values (inhibitor equilibrium dissociation constant) using the Cheng and Prusoff (1973) equation.

For some experiments, as indicated under *Results*, the shifts of the competitor versus [³H]QNB competition binding curve obtained in the absence or presence of 1 and 10 μM LY2033298 were fitted to the following form of a simple allosteric ternary complex model (Ehlert, 1988):

$$Y = \text{Bottom} + \frac{(\text{Top} - \text{Bottom}) \times [I]}{[I] + IC_{50} \left(\dfrac{1 + \dfrac{[B]}{K_B}}{1 + \alpha \dfrac{[B]}{K_B}} \right)} \tag{4}$$

where [I] denotes the concentration of competitor, IC_{50} denotes its potency in the absence of modulator, [B] denotes the concentration of LY2033298, K_B denotes the modulator equilibrium dissociation constant, and α denotes the "binding" cooperativity factor, which is a measure of the magnitude and direction of the allosteric effect the modulator exerts on the affinity of ligand I. Values of $\alpha > 1$ denote positive cooperativity, values < 1 (but greater than 0) denote negative cooperativity, values $= 1$ denote neutral cooperativity, and values approaching zero denote inhibition that is indistinguishable
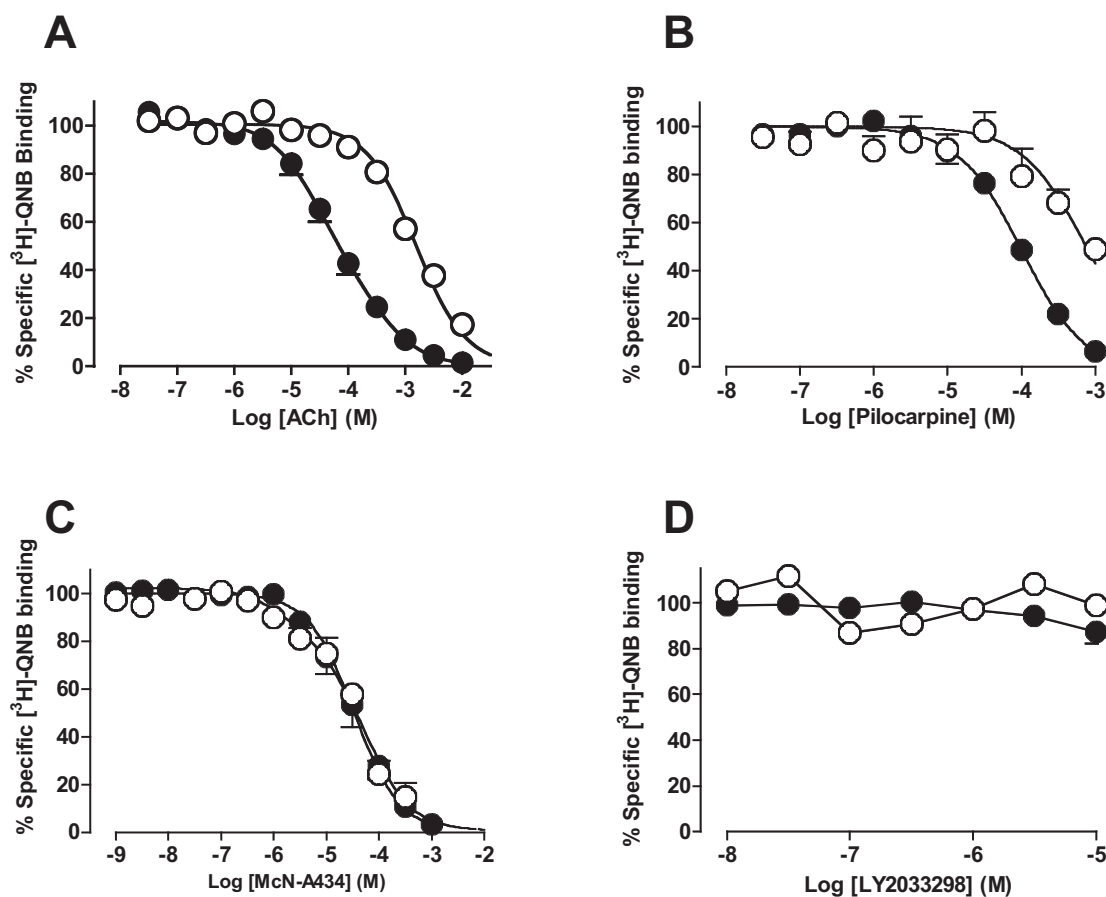
Fig. 2. Orthosteric and allosteric mAChR ligands display differential binding properties at the M_4 DREADD. Interaction between [³H]QNB and ACh (A), pilocarpine (B), McN-A-343 (C), or LY2033298 (D) at the WT M_4 mAChR (●) or the M_4 DREADD (○). All assays were performed in the presence of 100 μM GppNHp for 3 h at 37°C. The concentration of [³H]QNB was equal to its equilibrium dissociation constant at each receptor (0.09 and 6 nM for the M_4 mAChR and M_4 DREADD, respectively). Data points represent the mean ± S.E.M. of three to six experiments performed in triplicate.

from competitive (orthosteric) antagonism. This analysis also assumes that the interaction between the modulator and the radiolabel is neutrally cooperative ($\alpha = 1$), as was the case for the current study.

Concentration-response data generated from the ERK1/2 phosphorylation assays were normalized to the response generated by 10% FBS and fitted to the following three-parameter logistic equation:

$$E = \text{Bottom} + \frac{E_{\max} - \text{Bottom}}{1 + 10^{(-\text{pEC}_{50} - [A])}} \quad (5)$$

where E is response, $E_{\max}$ and Bottom are the top and bottom asymptotes of the curve, respectively, [A] is the agonist concentration, and pEC$_{50}$ is the negative logarithm of the agonist concentration that gives a response halfway between $E_{\max}$ and Bottom.

Functional experiments measuring the interaction between ACh and clozapine at the WT M$_4$ mAChR were globally fitted to the following logistic equation of agonist-antagonist interaction (Motulsky and Christopoulos, 2004):

$$\text{Response} = \text{Bottom} + \frac{(E_{\max} - \text{Bottom})}{1 + \left(\dfrac{10^{-\text{pEC}_{50}} [1 + ([B]/10^{-\text{p}A_2})^s]}{[A]}\right)} \quad (6)$$

where s represents the Schild slope for the antagonist, and pA_2 represents the negative logarithm of the concentration of antagonist that shifts the agonist EC$_{50}$ by a factor of 2; all other parameters are as defined in eq. 5.

For some of the functional interaction experiments, datasets were also fitted to the following operational model for the interaction between an agonist and allosteric modulator (Price et al., 2005; Leach et al., 2007):

$$E = \text{Basal}$$

$$+ \frac{E_{\text{m}}\tau_A^{n}[A]^n \left(1 + \dfrac{\alpha\beta[B]}{K_B}\right)^n}{\left[[A]\left(1 + \dfrac{\alpha[B]}{K_B}\right) + K_A\left(1 + \dfrac{[B]}{K_B}\right)\right]^n + \tau_A^{n}[A]^n \left(1 + \dfrac{\alpha\beta[B]}{K_B}\right)^n} \quad (7)$$

where E denotes the effect, A denotes the agonist, K_A denotes its equilibrium dissociation constant, B denotes the allosteric modulator, β denotes an empirical proportionality constant ("activation" cooperativity factor) that quantifies the change in stimulus imparted to the receptor by the agonist as a result of the presence of allosteric modulator, E_{m} denotes the maximum possible effect, τ_A is an operational measure of agonist (A) efficacy, and n is a "transducer" slope factor that governs the shape of the stimulus-response function. [A] and α are as defined above.

All parametric measures of potency, affinity, operational efficacy,

and cooperativity were estimated as logarithms (Christopoulos, 1998). Statistical comparisons between parameters were performed using Student's t test or F test, where appropriate, with $p < 0.05$ taken as indicating significance.

Results

The M$_4$ DREADD Displays Reduced Affinity for Prototypical Orthosteric Antagonists. Initial radioligand saturation binding studies used both the benzilate [³H]QNB and the tropate [³H]NMS as prototypical orthosteric mAChR antagonists. [³H]QNB bound with high affinity to the WT M$_4$ mAChR (pK_A 10.1 ± 0.1; $n = 3$), and detected a receptor expression level of 1.6 ± 0.2 pmol/mg of membrane protein. Y^{113}C and A^{203}G, the mutations responsible for generating the M$_4$ DREADD, led to a profound and significant ($p < 0.05$) decrease in the binding affinity of [³H]QNB (pK_A 8.2 ± 0.1; $n = 3$), as well as reduction in receptor expression (0.6 ± 0.1 pmol/mg), in keeping with our previous findings (Armbruster et al., 2007). [³H]NMS labeled a lower number of M$_4$ binding sites than [³H]QNB for both the WT (1.1 ± 0.2 pmol/mg; $n = 3$) and the DREADD (0.09 ± 0.04 pmol/mg; $n = 3$), possibly because of its hydrophilic nature, which does not allow it to access membrane-sequestered receptors. Similar to [³H]QNB, however, [³H]NMS also bound to the WT M$_4$ mAChR with much higher affinity (pK_A, 9.6 ± 0.1) than at the DREADD (pK_A, 7.3 ± 0.3).

The Nature of the Interacting Ligand Dictates Its Differential Affinity for the M$_4$ DREADD. Because [³H]QNB had higher affinity for both the WT and the DREADD than [³H]NMS, subsequent inhibition binding assays were performed using the benzilate as a probe of the orthosteric M$_4$ mAChR pocket. As shown in Fig. 2, A and B, the classic orthosteric agonists ACh and pilocarpine displayed a reduced potency for inhibiting [³H]QNB binding at the M$_4$ DREADD relative to the WT. Even though all experiments were performed in the presence of 100 μM GppNHp to promote receptor-G protein uncoupling, the binding of ACh at the WT could still be resolved into two apparent affinity states but reverted to a single low-affinity state at the DREADD (Table 1). Given that multiphasic agonist binding curves are common for high-affinity agonists and generally related to receptor-G protein coupling propensity (Kenakin, 1997), our finding suggests that the DREADD mutation may be affecting receptor-G protein coupling or conformational

TABLE 1

[³H]QNB inhibition binding parameters for various ligands at the wild type (WT) and DREADD M$_4$ mAChR.

Values represent the mean ± S.E.M. from n experiments performed in triplicate. ACh binding to the WT receptor could be resolved into two apparent dissociation constants. "High" and "Low" denote the negative logarithms of the apparent ligand dissociation constant for the high-and low-affinity states, respectively. Percentage high-affinity binding is shown in parentheses.

Ligand	M$_4$ WT		M$_4$ DREADD		n
	pK_B	n_H	pK_B	n_H	
ACh					
High	4.9 ± 0.2 (61 ± 23%)	0.8 ± 0.1	3.2 ± 0.1	0.8 ± 0.1	6
Low	3.9 ± 0.4				
Pilocarpine	4.3 ± 0.04	1.1 ± 0.1	3.4 ± 0.3*	0.8 ± 0.2	4
McN-A343	4.7 ± 0.1	0.9 ± 0.1	4.8 ± 0.1	0.7 ± 0.1	3
Clozapine	6.6 ± 0.1	0.8 ± 0.1	8.0 ± 0.1*	0.8 ± 0.2	6
CNO	4.9 ± 0.1	1.0 ± 0.3	6.6 ± 0.1*	0.8 ± 0.1	3
NDMC	6.0 ± 0.1	1.0 ± 0.1	7.4 ± 0.1*	1.2 ± 0.1	3

pK_B, the negative logarithm of the apparent ligand dissociation constant; n_H, Hill slope.
* Significantly different ($P < 0.05$) from the corresponding parameter at the M4 WT, as determined by Student's t test.

activation, in addition to direct effects on orthosteric ligand affinity.

It is noteworthy that when these experiments were repeated with McN-A-343 (Fig. 2C) or LY2033298 (Fig. 2D), a different profile of behaviors was noted. In particular, the binding of McN-A-343 was insensitive to the DREADD mutation (Table 1), a finding that is consistent with the hypothesis that this agonist uses a different mode of binding when interacting with mAChRs. Furthermore, LY203398 did not seem to interact at all with [³H]QNB over the concentration ranges tested, suggesting that the interaction between the modulator and this orthosteric antagonist is characterized by neutral cooperativity ($\alpha = 1$) at both the WT M_4 receptor and the DREADD; we could not use higher concentrations of the modulator because of solubility limits and nonspecific effects (not shown). In contrast, and in agreement with our initial study on the mAChR DREADDs (Armbruster et al., 2007), clozapine, CNO, and NDMC bound with significantly higher affinity to the M_4 DREADD than to the WT M_4 mAChR (Fig. 3, Table 1).

Allosteric Modulation by LY2033298 of Ligand Affinity Is Modified on the M_4 DREADD. To gain additional insight into the nature of allosteric interactions between the orthosteric and allosteric binding sites on the WT M_4 mAChR and the DREADD, additional competition binding studies were performed using ACh, clozapine, or CNO in the absence or presence of LY2033298. As shown in Fig. 4A, LY2033298 caused a robust and significant enhancement in the potency of ACh to inhibit [³H]QNB binding that was virtually lost at the M_4 DREADD (Fig. 4B). This finding clearly indicates that the positive cooperativity between ACh and LY2033298 is sensitive to the conformation of the orthosteric pocket, converting to neutral cooperativity at the M_4 DREADD. Interestingly, in these experiments the biphasic nature of ACh binding was retained at the DREADD, although the high affinity state represented a small fraction of the overall binding (Fig. 4B; Supplementary Table) in contrast to the WT, where the fraction of high affinity sites progressively increased with increasing modulator concentrations (Supplemental Table). Despite these complexities in the binding isotherms of ACh, and because the cooperativity between the allosteric modulator and the radioligand was neutral in all instances, we applied a simple allosteric ternary complex model to the LY2033298–mediated translocation of the ACh curves (eq. 4) to derive an approximation of the affinity of LY2033298 and its cooperativity with ACh at the WT receptor. This analysis yielded a value of $pK_B = 5.43 \pm 0.09$ ($n = 3$) and $\text{Log}\alpha = 1.78 \pm 0.06$ ($\alpha = 60$), which were in good agreement with our previous study of this interaction using [³H]NMS as the orthosteric probe (Chan et al., 2008).

When these experiments were repeated with either clozapine (Fig. 4, C and D) or CNO (Figs. 4, E and F) instead of ACh, very small effects were noted in the presence of LY2033298, with only a modest enhancement of inhibitor potency (Supplementary Table) at the highest concentration used (10 μM). The shifts were too small to allow application of eq. 4 unless we assumed a pK_B of 5.43 for LY2033298 at the WT receptor, in which case we could estimate a value of $\text{Log}\alpha = 0.65 \pm 0.05$ ($\alpha = 4.4$) for clozapine and 0.55 ± 0.05 ($\alpha = 3.5$) for CNO ($n = 3$). This weak interaction is either unaltered or slightly reduced at the M_4 DREADD (Figs. 4, D and F).

LY2033298 Is an Allosteric Agonist of M_4 mAChR-Mediated ERK1/2 Phosphorylation, and Its Efficacy Is Sensitive to the DREADD Mutations. Agonist-stimulated ERK1/2 phosphorylation was used as a measure of receptor activity to investigate the effects of the $Y^{113}C$ and $A^{203}G$ mutations on the function of the M_4 mAChR. In addition to the reduction in agonist affinity noted in our competition binding studies, both ACh and pilocarpine displayed a profound loss in the ability to stimulate ERK1/2 phosphorylation, as evidenced by a large reduction in potency (nearly 10,000-fold) and maximal effect for ACh and complete abolition of response to pilocarpine (Fig. 5, A and B; Table 2), in agreement with our prior findings (Armbruster et al., 2007).
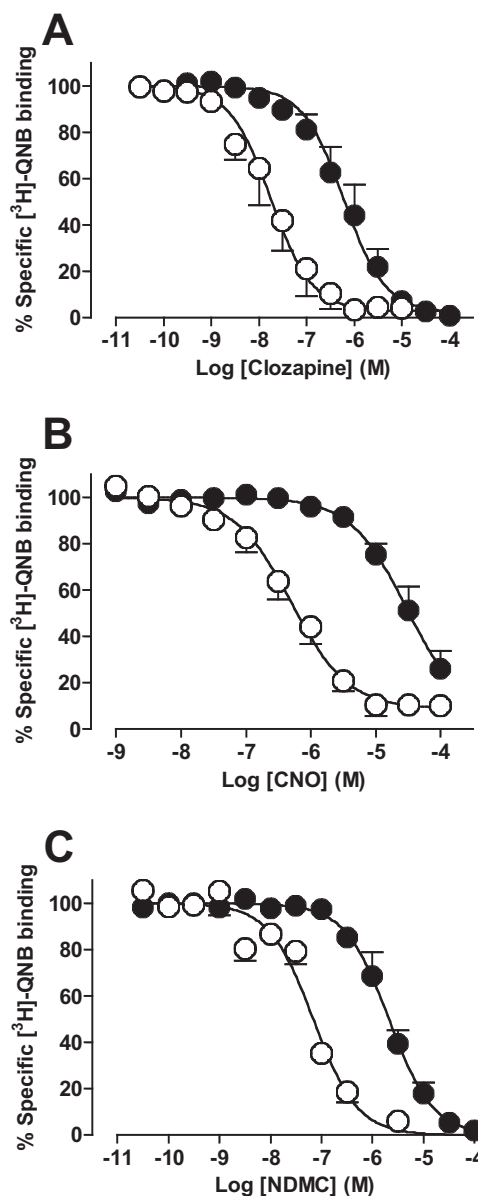
Fig. 3. Clozapine-like compounds have a higher affinity for the M_4 DREADD than the WT M_4 mAChR. Interaction between [³H]QNB and clozapine (A), CNO (B), or NDMC (C) at the WT M_4 mAChR (●) or the M_4 DREADD (○). All assays were performed in the presence of 100 μM GppNHp for 3 h at 37°C. The concentration of [³H]QNB was equal to its equilibrium dissociation constant at each receptor (0.09 and 6 nM for the M_4 mAChR and M_4 DREADD, respectively). Data points represent the mean ± S.E.M. of three to six experiments performed in triplicate.

It is noteworthy that McN-A-343, which was a more efficacious partial agonist than pilocarpine at the WT M$_4$ mAChR (Fig. 5C), also lost its ability to activate the M$_4$ DREADD despite having an unaltered affinity for the mutant receptor (Table 1). This finding suggests that the activating conformation McN-A-343 engenders is as sensitive to the DREADD mutations as those promoted by ACh and pilocarpine. To our surprise, we also discovered a novel property of LY2033298: the ability to act as a robust agonist of WT M$_4$ mAChR-mediated ERK1/2 phosphorylation in the absence of orthosteric ligand (Fig. 5D; Table 2). This is in contrast to our prior study, in which LY2033298 was either quiescent in the absence of orthosteric agonist for mediating intracellular calcium mobilization or only very weakly stimulated guanine nucleotide exchange on activated G proteins (Chan et al., 2008). Moreover, we found that the agonistic properties of LY2033298 were completely lost at the M$_4$ DREADD (Fig. 5D; Table 2), suggesting that LY2033298 has either a markedly reduced affinity for the allosteric site on the M$_4$ DREADD or, as with McN-A-343, that the activating conformation it engenders requires Tyr[113] and Ala[203] to be intact for transmission to the intracellular environment. In contrast, clozapine and its metabolites were converted from either inactive (clozapine, CNO) or very low efficacy (NDMC) ligands at the WT M$_4$ mAChR to efficacious and potent agonists at the M$_4$ DREADD (Fig. 6; Table 2).

Functional Interaction Studies Unmask Allosteric Effects on Agonist Efficacy and Reveal that LY2033298 Retains the Ability to Recognize an Allosteric Site on the M$_4$ DREADD. To investigate the potential for allosteric effects on agonist signaling efficacy, functional interaction studies between ligands were performed at both the WT M$_4$ mAChR and the M$_4$ DREADD. In the first instance, we investigated the effects of coaddition of ACh with LY2033298 at the WT M$_4$ mAChR. As shown in Fig. 7A, the major effect observed was an elevation in ERK1/2 phosphorylation owing
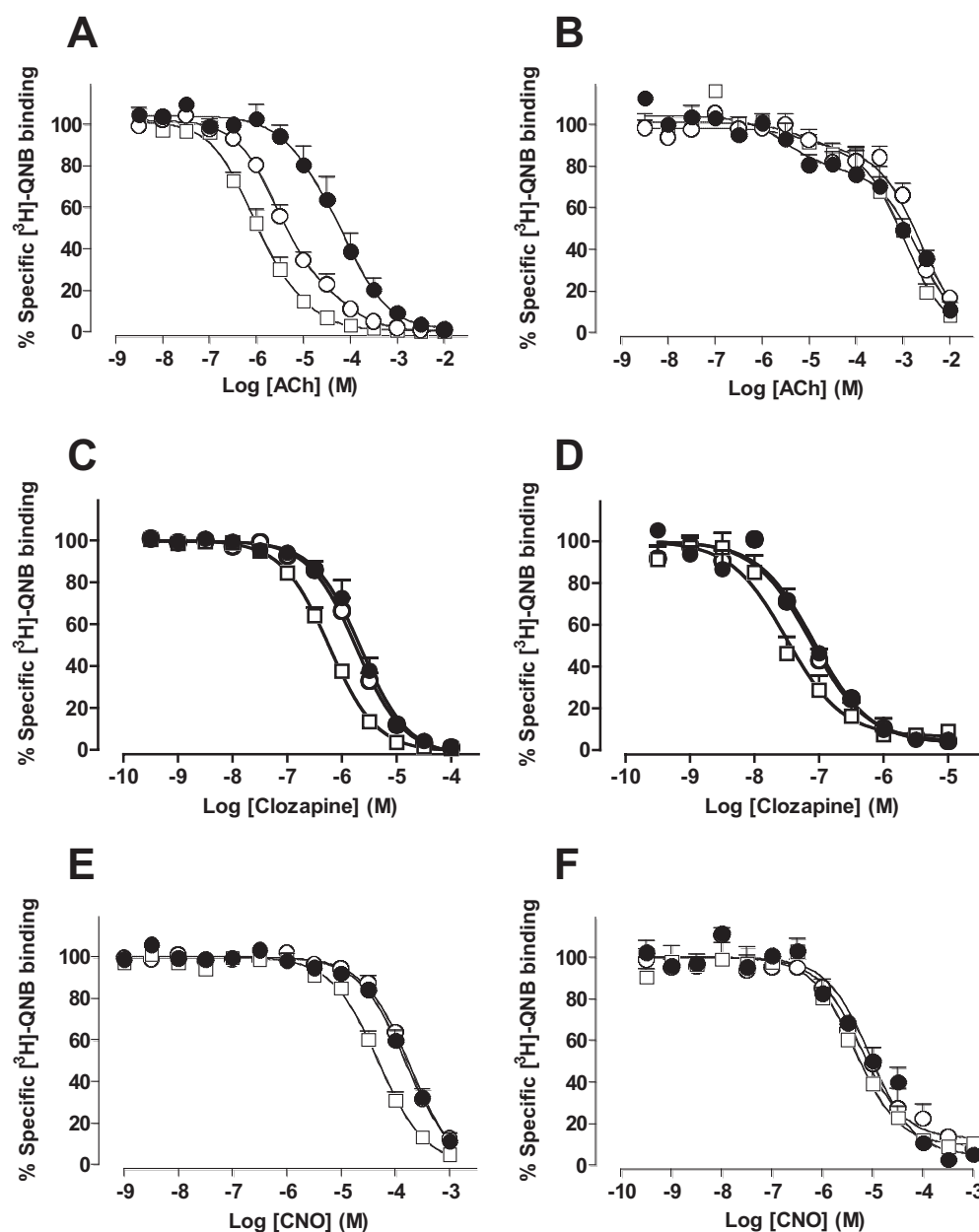
Fig. 4. The allosteric modulator LY2033298 displays altered cooperativity with orthosteric ligands at the M$_4$ DREADD. Interaction between [^{3}H]QNB and ACh (A and B), clozapine (C and D), or CNO (E and F) at the WT M$_4$ mAChR (A, C, E) or the M$_4$ DREADD (B, D, F) in the absence (●) or presence of 1 μM (○) or 10 μM (□) LY2033298. Data points represent the mean ± S.E.M. of three experiments performed in triplicate. All assays were performed in the presence of 100 μM GppNHp for 3 h at 37°C. The concentration of [^{3}H]QNB was equal to its equilibrium dissociation constant at each receptor (0.09 and 6 nM for the M$_4$ mAChR and M$_4$ DREADD, respectively).

to the intrinsic efficacy of LY2033298. No significant potentiation was noted in ACh potency at the highest concentration of LY2033298 used (1 μM), even though this concentration was sufficient to enhance ACh binding (Fig. 4A). A possible explanation for this discrepancy is a synergistic desensitization of the two ligands, which would offset any affinity-based gains in ACh potency by decreasing its efficacy; the reduction in ACh maximum response in the presence of 1 μM LY2033298 is also in agreement with this hypothesis. Alternatively, and given the variability in the data, it is possible that this observation simply reflects the difficulty in accurately determining ACh concentration-response curves as a result of the reduced system response window in the presence of high levels of receptor activation caused by LY2033298. In contrast, the interaction between clozapine and ACh at the WT M_4 mAChR exhibited behavior consistent with a simple competitive interaction (Fig. 7B). Application of eq. 6 to the data yielded a pA_2 estimate of 7.88 $\pm$ 0.08 (n = 3–6) for clozapine, which is in good agreement with other studies (http://pdsp.med.unc.edu) but is significantly higher ($p < 0.05$) than the corresponding estimate obtained from the

radioligand binding assays (6.6; Table 1); this discrepancy may be due to differences in the assay conditions for clozapine between the binding and functional experiments.

Because LY2033298 demonstrated agonistic properties at the WT M_4 mAChR, we were able to investigate its interactions with clozapine and CNO in a functional format for comparison with the modest (slightly positive) interaction noted in the binding interaction assays. As shown in Fig. 7, C and D, increasing concentrations of either clozapine or CNO resulted in a progressive reduction in the maximum agonist effect of LY2033298, clearly indicating a noncompetitive interaction. This finding suggests that the clozapine-like compounds exert a *negative allosteric effect* (*negative activation cooperativity*) on the intrinsic efficacy of LY2033298, despite their slightly positive binding cooperativity. We attempted to quantify this negative activation cooperativity by fitting an operational model of allosterism (eq. 7) to the data in Fig. 7, C and D. Because of the large number of model parameters, we fixed the estimates of pK_A (agonist affinity) and Logα (cooperativity) to the corresponding values for LY2033298 determined in the interaction binding studies. The remaining

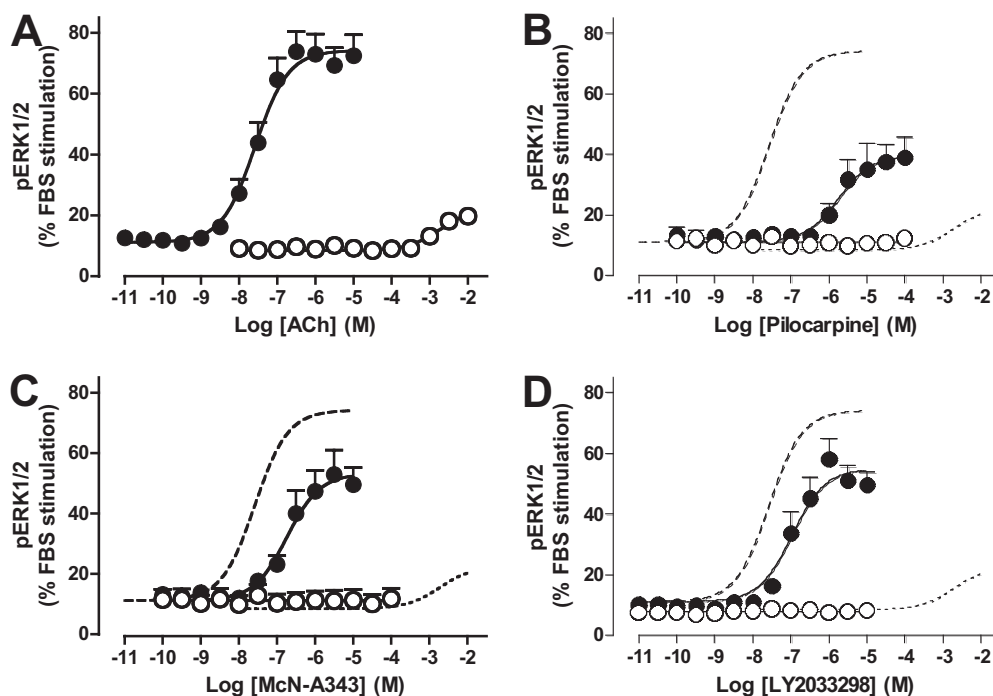**Fig. 5.** Orthosteric and allosteric mAChR agonists lose efficacy at the M_4 DREADD. Concentration-response curves of ERK1/2 phosphorylation for ACh (A), pilocarpine (B), McN-A-343 (C), or LY2033298 (D) at 37°C in CHO FlpIn cells stably expressing the WT M_4 mAChR (●) or the M_4 DREADD (○). Dashed lines in B to D show the corresponding responses to ACh for comparison. Data points represent the mean $\pm$ S.E.M. of four to seven experiments performed in triplicate.

TABLE 2
Concentration-response curve potency (pEC_{50}) and maximal agonist response (E_{max}) parameters for agonist-stimulated phosphorylation of ERK1/2 at the WT and DREADD M_4 mAChR
Values represent the mean $\pm$ S.E.M. from n experiments performed in triplicate.

Ligand	M_4 WT		M_4 DREADD		n
	pEC_{50}	E_{max}	pEC_{50}	E_{max}	
ACh	7.6 $\pm$ 0.1	74 $\pm$ 2	2.7 $\pm$ 0.4*	23 $\pm$ 5*	7
Pilocarpine	5.7 $\pm$ 0.3	40 $\pm$ 4	N.D.	N.D.	4
McN-A-343	6.7 $\pm$ 0.1	53 $\pm$ 3	N.D.	N.D.	7
LY2033298	7.0 $\pm$ 0.1	55 $\pm$ 2	N.D.	N.D.	7
Clozapine	N.D.	N.D.	8.4 $\pm$ 0.1	53 $\pm$ 1	7
CNO	N.D.	N.D.	7.0 $\pm$ 0.1	45 $\pm$ 2	7
NDMC	6.8 $\pm$ 0.7	19 $\pm$ 3	8.0 $\pm$ 0.1*	42 $\pm$ 1*	7

pEC_{50}, negative logarithm of the EC_{50}; E_{max}, maximal agonist-stimulated response, expressed as a percentage of the response stimulated by 10% FBS;, N.D., not determined.
* Significantly different ($P < 0.05$) from the corresponding parameter at the M4 WT, as determined by Student's t test.

model parameters were estimated by nonlinear regression, and the results are shown in Table 3, where a number of features can be noted. First, the functional estimate of the affinity (pK_B) of clozapine as an allosteric antagonist of LY2033298 is in excellent agreement with the pA_2 value obtained for clozapine's competitive interaction with ACh under the same functional assay conditions; this is consistent with the fact that clozapine should be mediating both these effects (orthosteric competition with ACh; allosteric modulation with LY2033298) from the same binding site. Second, a pK_B estimate for CNO as an allosteric modulator of LY2033298 efficacy was also obtained. Third, the estimates of logβ for both ligands were highly negative; with respect to

CNO, the nonlinear regression trended toward a boundary value, indicating that the parameter was practically indistinguishable from $\beta = 0$ and could thus not be estimated accurately. This is consistent with the notion that the efficacy modulation is so highly negative that LY2033298 is incapable of generating a stimulus on a receptor occupied by clozapine-like compounds.

Finally, we performed interaction studies on the M$_4$ DREADD. The most striking result was obtained when LY2033298 was coadministered with ACh. Figure 8A shows that, despite losing agonistic properties, LY2033298 was able to "rescue" ACh potency and efficacy at the otherwise functionally inactive M$_4$ DREADD, providing conclusive evidence for the presence of an allosteric site on this mutant receptor that retained the capacity to modulate orthosteric functionality. Furthermore, application of our operational model of allosterism to the data set yielded the parameters shown in Table 3, where it can be seen that the functional estimate of ACh affinity is in good agreement with the corresponding value from the radioligand binding assays (Table 1). Furthermore, and of importance, we also obtained an estimate of the affinity of LY2033298 for the DREADD, which we were unable to do from the binding studies. The LY2033298 pK_B value of 5.39 for the DREADD is very similar to the value determined for the WT M$_4$ mAChR (5.43), indicating that the affinity of LY2033298 for the allosteric site is not affected by the Y[113]C and A[203]G mutations in the orthosteric pocket. However, the cooperativity between ACh and LY2033298 changed dramatically on the DREADD. Because the radioligand binding studies indicated a neutral cooperativity at the level of binding affinity between the two at the DREADD (Fig. 4B; Logα = 0), the functional rescue by LY2033298 of ACh signaling must be totally due to positive activation cooperativity. In our model, this is quantified by the parameter logβ, which indicated a greater than 100-fold enhancement in the efficacy of ACh by LY2033298. In contrast, LY2033298 did not appreciably affect the potency or maximum response of either clozapine or CNO as agonists at the DREADD receptor (Fig. 8, B and C), indicating neutral cooperativity with these DREADD agonists.

Discussion

This study provides new evidence for conformational flexibility in the function of the M$_4$ mAChR. By using structurally diverse orthosteric ligands such as ACh and the clozapine-like molecules on a reverse-engineered M$_4$ DREADD, we identified differential effects on binding and signaling that suggest multiple modes of receptor engagement. Furthermore, through analysis of the actions of a novel allosteric agonist/modulator, LY2033298, we provide evidence for the retention of an allosteric site on the M$_4$ DREADD that has altered modes of cooperativity with the orthosteric site compared with the WT but can still restore functionality to an otherwise unresponsive receptor. Given that allosteric ligands are increasingly being discovered for many other GPCRs, these findings are likely to have relevance beyond the mAChR family.

Radioligand binding assays found that the M$_4$ DREADD had reduced affinity for orthosteric antagonists, such as [^{3}H]-QNB and [^{3}H]NMS, as well as for classic orthosteric agonists such as ACh and pilocarpine. In contrast, clozapine and its two metabolites, CNO and NDMC, showed an increase in

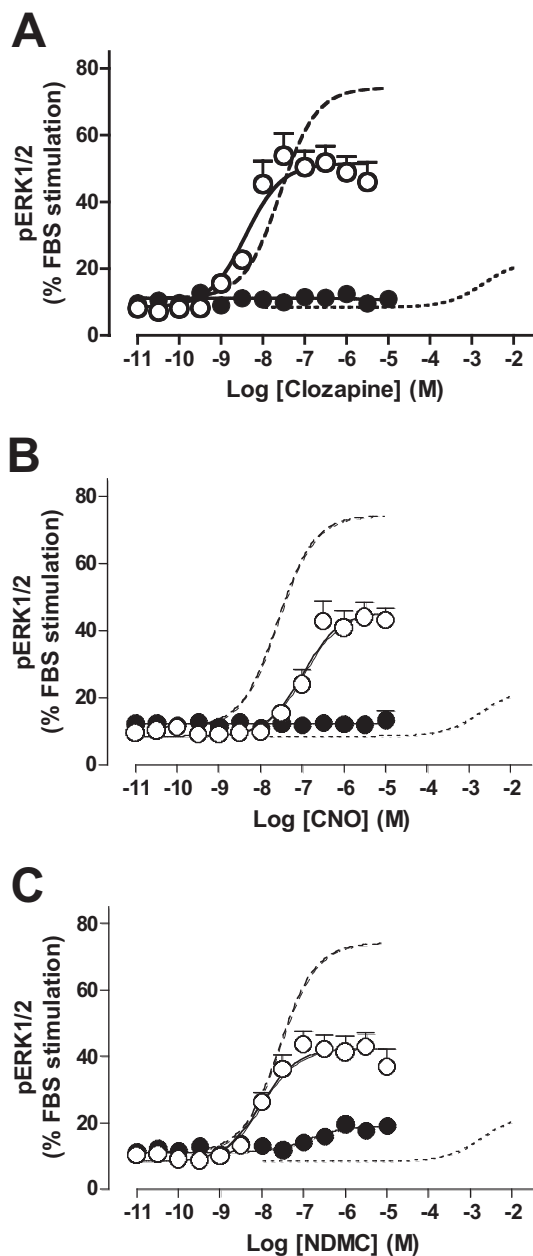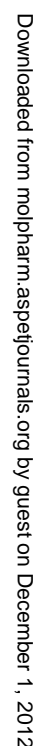**Fig. 6.** Clozapine-like compounds gain efficacy at the M$_4$ DREADD. Concentration-response curves of ERK1/2 phosphorylation for clozapine (A), CNO (B), or NDMC (C) at 37°C in CHO FlpIn cells stably expressing the WT M$_4$ mAChR (●) or the M$_4$ DREADD (○). Dashed lines show the corresponding responses to ACh (Fig. 5A) for comparison. Data points represent the mean ± S.E.M. of seven experiments performed in triplicate.

binding affinity. These findings are the first to demonstrate that the divergent effects of the DREADD mutations on the function of ACh-like compounds, on the one hand, and clozapine-like compounds, on the other (Armbruster et al., 2007), are due in part to changes in binding affinity. Additional insights were gained from investigation of mAChR ligands believed to act allosterically. McN-A-343 is a partial agonist suggested either to act solely through an allosteric site (Birdsall et al., 1983) or to recognize both orthosteric and allosteric sites on the M_2 mAChR (Waelbroeck, 1994; May et al.,

2007a). The fact that its affinity was unaltered at the M_4 DREADD (Fig. 2C, Table 1) is consistent with a nonclassical mode of binding compared with ACh, but further experiments are required to conclusively address the nature of the interaction between McN-A-343 and the M_4 mAChR. In contrast, the novel modulator LY2033298 did not seem to interact with the orthosteric antagonist [^{3}H]QNB at either the WT M_4 mAChR or the DREADD. Given that positive cooperativity could be demonstrated between this compound and ACh in binding ($\alpha = 60$) at the WT M_4 mAChR (Fig. 4A) and

Fig. 7. The orthosteric agonist, ACh, and the allosteric agonist, LY2033298, display different interactive properties at the WT M_4 mAChR. Concentration-response curves of ERK1/2 phosphorylation at 37°C in CHO FlpIn cells stably expressing the WT M4 mAChR for ACh (A and B) or LY2033298 (C and D) in the absence (●) or presence of 0.1 μM (○), 1 μM (□) or 10 μM (◇) of A) LY2033298 (A), clozapine (B and C), or CNO (D). Curves drawn through the data in B represent the best global fit of a competitive model of interaction (eq. 6). Curves drawn through the data in C and D represent the best global fit of an operational model of allosterism (eq. 7). Data points represent the mean + S.E.M. of three to six experiments performed in triplicate.

TABLE 3
Operational model parameters for the allosteric interaction between LY2033298 and various ligands at either the wild type (WT) or DREADD M_4 mAChR

Except as indicated otherwise, parameter values represent the mean ± S.E.M. from three to six experiments performed in triplicate. The letters in parentheses denote corresponding ligands in the operational model (eq. 7; A = agonist; B = modulator).

Parameter	LY2033298 (A) vs Clozapine (B) M_4 WT	LY2033298 (A) vs CNO (B) M_4 WT	ACh (A) vs LY2033298 (B) M_4 DREADD
pK_A	5.43[a]	5.43[a]	3.53 ± 0.19
pK_B	7.87 ± 0.17	6.07 ± 0.09	5.39 ± 0.73
Log α	0.65[a]	0.55[a]	0[a]
Log β	−2.61 ± 0.83	N.F.	2.19 ± 0.81
	($\beta = 0.002$)	($\beta \to 0$)	($\beta = 155$)
Log τ_A	1.66 ± 0.13	1.56 ± 0.07	0.38 ± 0.12
E_m	47.1 ± 4.7	69.0 ± 3.8	53.7 ± 2.9
n	1.52 ± 0.46	1.36 ± 0.49	1.63 ± 0.36

pK_A, negative logarithm of the dissociation constant of ligand A (agonist); pK_B, negative logarithm of the dissociation constant of ligand B (modulator); Log α, logarithm of the binding cooperativity factor; Log β, logarithm of the activation cooperativity factor; Log τ_A, logarithm of the agonist operational efficacy parameter; E_m, maximum system response level; n, transducer slope factor; N.F., not fitted; parameter estimate was ambiguous and approached a lower boundary (less than −90), indicating that the value of β was practically indistinguishable from zero.
[a] Fixed as a constant based on the value determined in the radioligand binding assay.

signaling ($\beta = 155$) at the DREADD (Fig. 8A; Table 3), the lack of interaction with [^{3}H]QNB is indicative of neutral binding cooperativity ($\alpha = 1$) at both receptors.

In addition to the varied pattern of effects noted for the DREADD mutations on ligand affinities, different behaviors were observed on ligand efficacies in functional assays of ERK1/2 phosphorylation. As anticipated, ACh and pilocarpine had markedly reduced potencies and maximal responses at the DREADD relative to the WT M$_4$ mAChR. In addition, the clozapine-like compounds displayed the opposite properties at the DREADD, namely a gain of functional potency and efficacy. Most surprising, however, were the findings with LY2033298, which displayed agonistic properties at the WT receptor; we had not detected appreciable

Fig. 8. LY2033298 rescues ACh function at the M$_4$ DREADD but does not interact functionally with clozapine-like compounds. Concentration-response curves of ERK1/2 phosphorylation at 37°C in CHO FlpIn cells stably expressing the WT M$_4$ mAChR for ACh (A), clozapine (B), or CNO (C) in the absence (●) or presence of 0.03 (▽), 0.1 (○), 0.3 (△), 1 (□), or 10 μM (◇) LY2033298. Curves drawn through the data in A represent the best global fit of an operational model of allosterism (eq. 7). Data points represent the mean + S.E.M. of three to six experiments performed in triplicate.

levels of agonism in our initial characterization of this compound using intracellular calcium mobilization or guanine nucleotide exchange as functional readouts (Chan et al., 2008). This result may be due to differences in receptor-effector coupling between the cell lines used in our studies (CHO FlpIn versus CHO-K1) or due to LY2033298 trafficking receptor stimulus to the ERK1/2 pathway as opposed to classic pathways such as calcium mobilization or nucleotide exchange. Further studies are currently under way to address this issue. However, the agonist activity of both LY2033298 and McN-A-343 was lost upon mutation of Y^{113}C and A^{203}G, and this was not due to a loss in binding affinity at the M$_4$ DREADD. Therefore, there are two important implications of these findings. First, because Tyr^{113} and Ala^{203} are located in the orthosteric binding pocket, these residues could directly affect the binding of prototypical orthosteric compounds, such as ACh, pilocarpine, and [^{3}H]QNB, but have a minimal effect on the binding of ligands such as LY2033298 and McN-A-343. The fact that clozapine and its metabolites *gain* affinity at the DREADD suggests that they adopt a different orientation within the orthosteric site relative to ACh, such that the mutation of Tyr^{113} and Ala^{203} leads to a gain in the free energy of binding for clozapine-like molecules. The second major implication is that, in addition to their involvement in ligand binding, Tyr^{113} and Ala^{203} must be involved in a conformational switch that links receptor occupancy to activation. Moreover, this conformational switch is not restricted to prototypical orthosteric ligands but is also part of the network that atypical agonists such as LY2033298 and McN-A-343 use to transmit their signal via the receptor to the cell.

Subsequent experiments focused on the interactive properties between orthosteric and allosteric sites on the M$_4$ mAChR to determine whether the magnitude and direction of allosteric modulation was also affected by the DREADD mutation. The ability of LY2033298 to bind to a topographically distinct site as an allosteric modulator was readily apparent in radioligand binding assays of the WT M$_4$ mAChR, where LY2033298 caused a concentration-dependent leftward translocation of the ACh/[^{3}H]QNB competition binding curve (Fig. 4A). Application of an allosteric model to the data yielded affinity and cooperativity estimates for the interaction that were in general agreement with our previous study (Chan et al., 2008), although we acknowledge that the nature of the interaction at the molecular level is more complex because the modulator, in this instance, seemed to affect the proportion of high-affinity states for ACh in addition to its affinity. In contrast, the cooperativity was only weakly positive with clozapine and CNO, highlighting the fact that allosteric interactions can be highly probe-dependent (Leach et al., 2007). Additional evidence for an allosteric mechanism of LY2033298 action at the WT M$_4$ mAChR was obtained when it was tested against clozapine and CNO in functional assays of ERK1/2 phosphorylation, where increasing concentrations of either clozapine or CNO markedly reduced the efficacy of LY2033298; in our operational model of allosterism, this is reflected in values of the activation cooperativity parameter, β, trending toward zero (Table 3), even though the binding cooperativity parameter, α, is (albeit only slightly) greater than 1. Differential effects on binding cooperativity, on the one hand, and activation cooperativity, on the other, have previously been noted for other allosteric
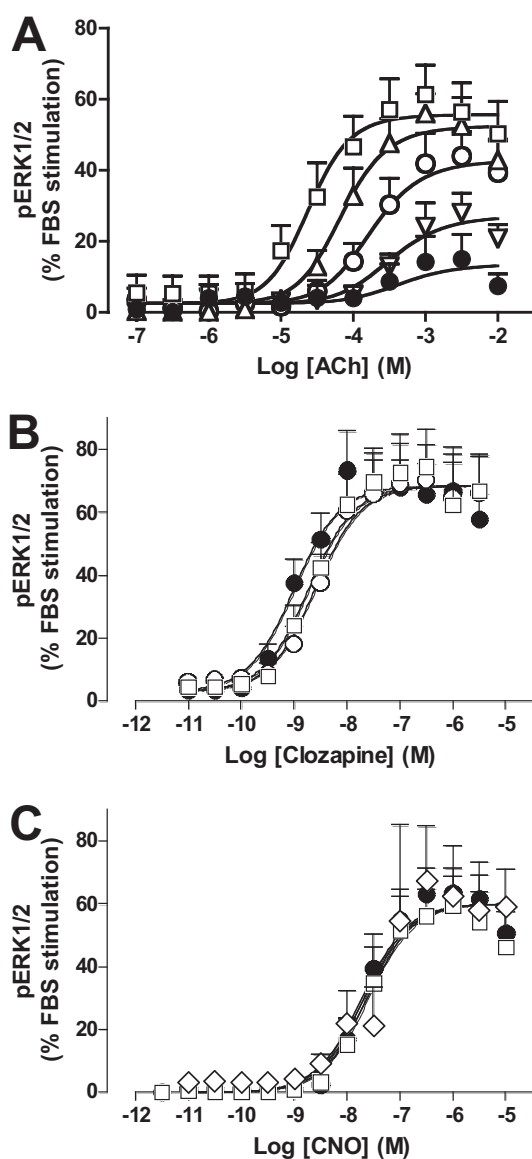
modulators of GPCRs (Christopoulos, 2002) and highlight the need to study allosteric modulator actions in a variety of different assay formats.

When interaction experiments were repeated on the DREADD, it became readily apparent that the mutations had a profound effect on the cooperativity between the orthosteric and allosteric sites. The most striking finding was that despite both ACh and LY2033298 losing their agonistic effects at the M_4 DREADD, the combination of the two led to a significant functional rescue of ACh potency and efficacy (Fig. 8A). This finding clearly demonstrates that LY2033298 is still able to bind to the M_4 DREADD (with similar affinity as for the WT; Table 3) and act as an allosteric modulator of the orthosteric site, even though it can no longer act as an allosteric agonist. In addition, the nature of the allosteric interaction on the DREADD seems totally driven by positive activation cooperativity, because radioligand binding studies revealed neutral binding cooperativity between ACh and LY2033298 on the DREADD in contrast to the positive cooperativity observed at the WT receptor (Fig. 4B). Perhaps most importantly, this finding has also identified another novel approach to exploiting DREADDs; although we have no reason to assume that activation of the DREADD by an exogenous ligand (e.g., CNO) does not faithfully recapitulate the signaling properties of the native mAChR, our ability to now engender responsiveness to the *native agonist* by using an allosteric modulator such as LY2033298 provides a new opportunity to directly address this assumption.

Because the allosteric interaction between LY2033298 and the clozapine-like compounds at the WT M_4 mAChR was different from that between the modulator and ACh, it was perhaps not so surprising that the DREADD mutation led to a different clozapine/CNO-LY2033298 interaction compared with ACh. In this case, however, the interaction between either clozapine or CNO and LY2033298 was characterized by a neutral activation cooperativity; i.e., the effect of the DREADD mutation seemed to be a functional "uncoupling" of the allosteric site and the orthosteric site when the latter is used by clozapine-like molecules. This is further evidence that the transmission of cooperative effects between orthosteric and allosteric sites on the M_4 mAChR relies on the complementarity between specific molecules and their attachment points, as well as conformational cross-talk between the two sites. Figure 9 summarizes the main elements of our findings for ACh and CNO in schematic form, although it should be noted that this is not intended to represent a model for the underlying molecular mechanisms governing the observed behaviors. Indeed, the observed affinity modulation by LY2033298 of ACh at the WT M_4, as well as the efficacy modulation at the DREADD, may reflect a common molecular mechanism at both receptors, whereby LY2033298 allosterically promotes an active receptor state that would
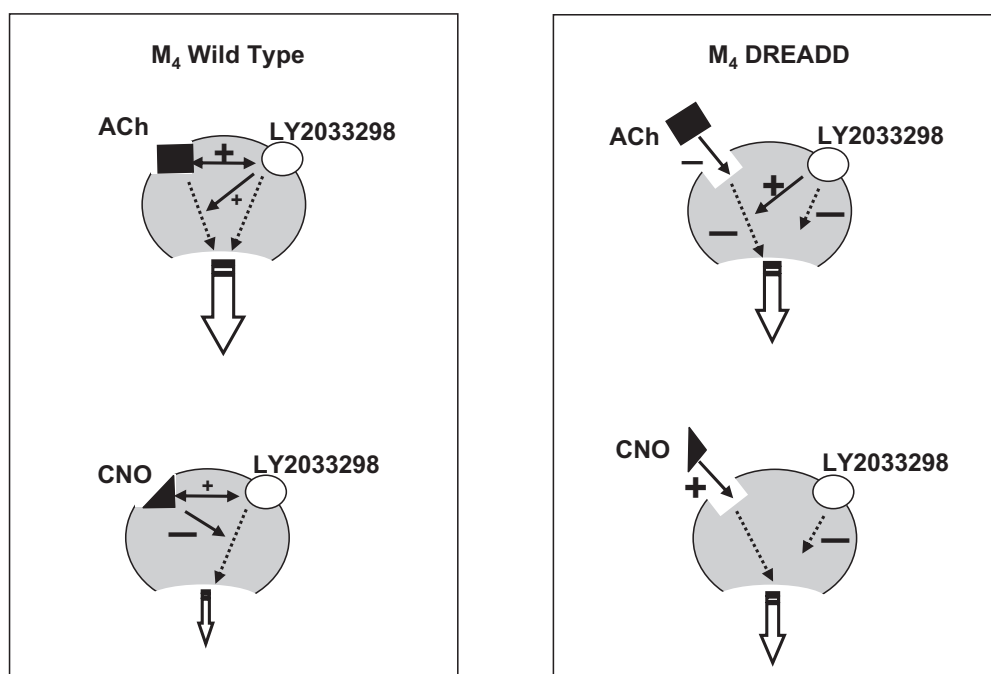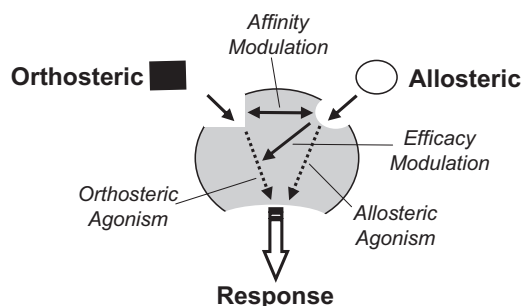

Fig. 9. The DREADD mutations change the nature of ligand interaction with the M_4 mAChR and the transmission of cooperative effects between the two sites. Scheme highlighting the interactions between LY2033298 and either ACh or CNO at the WT and DREADD M_4 mAChRs. Positive allosteric modulation is highlighted by +, whereas negative allosteric modulation is indicated by −.

manifest as an increase in apparent affinity for a highly efficacious agonist (ACh at the M$_4$ WT) but an increase in efficacy for a low efficacy agonist (ACh at the M$_4$ DREADD; see Ehlert and Griffin, 2008).

In conclusion, this study has used a novel pharmacological probe, LY2033298, and a novel biological tool, the M$_4$ DREADD, to gain new insights into the molecular pharmacology of the M$_4$ mAChR. We have found that Tyr[113] and Ala[203] are not only involved in the binding and activation mechanism of orthosteric mAChR ligands but also participate in the activation and cooperative mechanisms of allosteric ligands. The finding that LY2033298 can rescue function of an endogenous ligand at a mutationally impaired receptor also has significant relevance for the potential development of allosteric modulators for diseases in which receptor mutations cause decreased orthosteric activity; if the allosteric site remains intact, it can be used as an alternative drug target. Improved understanding of the structure-function relationships of both orthosteric and allosteric GPCR sites may thus be used for the development of more selective therapeutics for a number of disorders.

References

Armbruster BN, Li X, Pausch MH, Herlitze S, and Roth BL (2007) Evolving the lock to fit the key to create a family of G protein-coupled receptors potently activated by an inert ligand. *Proc Natl Acad Sci U S A* **104:**5163–5168.

Birdsall NJ, Burgen AS, Hulme EC, Stockton JM, and Zigmond MJ (1983) The effect of McN-A-343 on muscarinic receptors in the cerebral cortex and heart. *Br J Pharmacol* **78:**257–259.

Bishop A, Buzko O, Heyeck-Dumas S, Jung I, Kraybill B, Liu Y, Shah K, Ulrich S, Witucki L, Yang F, et al. (2000) Unnatural ligands for engineered proteins: new tools for chemical genetics. *Annu Rev Biophys Biomol Struct* **29:**577–606.

Bradford MM (1976) A rapid and sensitive method for the quantitation of microgram quantities of protein utilizing the principle of protein-dye binding. *Analyt Biochem* **72:**248–254.

Chan WY, McKinzie D, Bose S, Mitchell S, Witkin J, Thompson RC, Christopoulos A, Lazareno S, Birdsall NJM, Bymaster FP and CC Felder (2008) Allosteric modulation of the muscarinic M$_4$ receptor as a novel approach to treating schizophrenia. *Proc Natl Acad Sci U S A* **105:**10978–10983.

Cheng Y and Prusoff WH (1973) Relationship between the inhibition constant (K$_I$) and the concentration of inhibitor which causes 50 per cent inhibition (I$_{50}$) of an enzymatic reaction. *Biochem Pharmacol* **22:**3099–3108.

Christopoulos A (1998) Assessing the distribution of parameters in models of ligand-receptor interaction: to log or not to log. *Trends Pharmacol Sci* **19:**351–357.

Christopoulos A (2002) Allosteric binding sites on cell-surface receptors: novel targets for drug discovery. *Nat Rev Drug Discov* **1:**198–210.

Christopoulos A and Kenakin T (2002) G protein-coupled receptor allosterism and complexing. *Pharmacol Rev* **54:**323–374.

Davies MA, Compton-Toth BA, Hufeisen SJ, Meltzer HY, and Roth BL (2005) The highly efficacious actions of *N*-desmethylclozapine at muscarinic receptors are unique and not a common property of either typical or atypical antipsychotic drugs: is M$_1$ agonism a pre-requisite for mimicking clozapine's actions? *Psychopharmacology* **178:**451–460.

Ehlert FJ (1988) Estimation of the affinities of allosteric ligands using radioligand binding and pharmacological null methods. *Mol Pharmacol* **33:**187–194.

Ehlert FJ and Griffin MT (2008) Two-state models and the analysis of the allosteric effect of gallamine at the M$_2$ muscarinic receptor. *J Pharmacol Exp Ther* **325:**1039–1060.

Felder CC, Chan WY, Broad L, Lazareno S, Birdsall NJ, Bose S, Mitchell S, Large T, Emkey R, Sher E, et al. (2004) Pharmacological and molecular characterization of a positive allosteric modulator selective for the muscarinic M4 receptor being developed for treatment of psychosis (Abstract). *Neuropsychopharmacology* **29 (Suppl S1):**S115.

Gregory KJ, Sexton PM, and Christopoulos A (2007) Allosteric modulation of muscarinic acetylcholine receptors. *Curr Neuropharmacol* **5:**157–167.

Kenakin TP (1997) *Pharmacologic Analysis of Drug-Receptor Interaction.* Lippincott-Raven, Philadelphia, PA.

Leach K, Sexton PM, and Christopoulos A (2007) Allosteric GPCR modulators: taking advantage of permissive receptor pharmacology. *Trends Pharmacol Sci* **28:**382–389.

May LT, Avlani VA, Langmead CJ, Herdon HJ, Wood MD, Sexton PM, and Christopoulos A (2007a) Structure-function studies of allosteric agonism at M2 muscarinic acetylcholine receptors. *Mol Pharmacol* **72:**463–476.

May LT, Leach K, Sexton PM, and Christopoulos A (2007b) Allosteric Modulation of G Protein-Coupled Receptors. *Annu Rev Pharmacol Toxicol* **47:**1–51.

Motulsky and Christopoulos (2004) *Fitting Models to Biological Data Using Linear and Nonlinear Regression. A Practical Guide to Curve-Fitting.* Oxford University Press, New York.

Price MR, Baillie GL, Thomas A, Stevenson LA, Easson M, Goodwin R, McLean A, McIntosh L, Goodwin G, Walker G, et al. (2005) Allosteric modulation of the cannabinoid CB1 receptor. *Mol Pharmacol* **68:**1484–1495.

Scearce-Levie K, Coward P, Redfern CH, and Conklin BR (2001) Engineering receptors activated solely by synthetic ligands (RASSLs). *Trends Pharmacol Sci* **22:**414–420.

Shirey JK, Xiang Z, Orton D, Brady AE, Johnson KA, Williams R, Ayala JE, Rodriguez AL, Wess J, Weaver D, et al. (2008) An allosteric potentiator of M4 mAChR modulates hippocampal synaptic transmission. *Nat Chem Biol* **4:**42–50.

Sur C, Mallorga PJ, Wittmann M, Jacobson MA, Pascarella D, Williams JB, Brandish PE, Pettibone DJ, Scolnick EM, and Conn PJ (2003) desmethylclozapine, an allosteric agonist at muscarinic 1 receptor, potentiates *N*-methyl-D-aspartate receptor activity. *Proc Natl Acad Sci U S A* **100:**13674–13679.

Waelbroeck M (1994) Identification of drugs competing with *d*-tubocurarine for an allosteric site on cardiac muscarinic receptors. *Mol Pharmacol* **46:**685–692.

Wess J, Duttaroy A, Zhang W, Gomeza J, Cui Y, Miyakawa T, Bymaster FP, McKinzie L, Felder CC, Lamping KG, et al. (2003) M1–M5 muscarinic receptor knockout mice as novel tools to study the physiological roles of the muscarinic cholinergic system. *Recept Channels* **9:**279–290.

Wess J, Eglen RM, and Gautam D (2007) Muscarinic acetylcholine receptors: mutant mice provide new insights for drug development. *Nat Rev Drug Discov* **6:**721–733.

Address correspondence to: Prof. Arthur Christopoulos, Drug Discovery Biology Laboratory, Department of Pharmacology, Monash University, Clayton, Victoria 3800, Australia. E-mail: arthur.christopoulos@med.monash.edu.au